Journal of the Geological Society

Ammonoid recovery after the Permian–Triassic mass extinction: a re-exploration of morphological and phylogenetic diversity patterns

Morgane Brosse, Arnaud Brayard, Emmanuel Fara and Pascal Neige

Journal of the Geological Society 2013, v.170; p225-236.
doi: 10.1144/jgs2012-084

Notes

Journal of the Geological Society, London, Vol. **170**, 2013, pp. 225–236. doi: 10.1144/jgs2012-084.

Ammonoid recovery after the Permian–Triassic mass extinction: a re-exploration of morphological and phylogenetic diversity patterns

MORGANE BROSSE[1,2]*, ARNAUD BRAYARD[1], EMMANUEL FARA[1] & PASCAL NEIGE[1]
[1]*UMR CNRS 6282 Biogéosciences, Université de Bourgogne, 6 Boulevard Gabriel, F-21000, Dijon, France*
[2]*Paläontologisches Institut und Museum, Universität Zürich, Karl-Schmid Strasse 4, CH-8006 Zürich, Switzerland*
**Corresponding author (e-mail: morgane.brosse@pim.uzh.ch)*

Abstract: The explosive ammonoid rediversification after the Permian–Triassic mass extinction is now well understood in terms of taxonomic richness and biogeography. Using an updated dataset of Early Triassic ammonoids, we compare morphological disparity and taxonomic richness patterns at the regional and global scales. Disparity evolved similarly at both scales, suggesting a global influence of abiotic factors. Morphological diversification occurred early in the Smithian and a marked contraction of the morphospace took place during the end-Smithian extinction. We confirm that trends in disparity and richness were decoupled during the Griesbachian and Dienerian. Three macroevolutionary processes may be involved: (1) a nonselective extinction at the Permian–Triassic boundary; (2) a Dienerian constrained radiation with several homeomorphic genera; (3) a potential deterministic extinction during the end-Smithian crisis. We also demonstrate a superfamily imprint upon disparity for the Spathian when most superfamilies occupied a restricted part of the morphospace. Sphaerocones were the most affected by the Dienerian and end-Smithian extinction, but explanations remain elusive. On the one hand, this may be linked to widespread harsh conditions at those times. On the other hand, as the sphaerocones occurred episodically during the Early Triassic, this might be explained by a relaxing of ecological constraints or simply by convergent evolution.

Supplementary materials: The database, including measurements of specimens illustrated in previously published plates and of unpublished specimens from Utah, South China and Spiti, as well as the number of genera present in each studied substage of the Early Triassic, are available at www.geolsoc.org.uk/SUP18571.

The Permian–Triassic (PT) crisis was the largest mass extinction of the past 600 Ma and was marked by the disappearance of almost all typical Palaeozoic organisms (e.g. trilobites, rugose and tabulate corals, fusulinid foraminifers). About 90% of all marine species on Earth disappeared during this event (Raup 1979). It is usually assumed that the PT mass extinction provides a classic example of a long delay before the onset of the subsequent biotic recovery (e.g. Erwin 2001). Indeed, both continental and marine communities throughout the Early Triassic seemed to be characterized by low-diversity assemblages and opportunistic, cosmopolitan taxa (e.g. Schubert & Bottjer 1992; Erwin 2001; Rodland & Bottjer 2001). However, later studies on benthic foraminifers (Song *et al*. 2011), trace fossils (e.g. Hofmann *et al*. 2011) and metazoan bioconstructions (Brayard *et al*. 2011) have suggested that the rediversification and restructuring of benthic communities was perhaps more rapid than traditionally thought, opening numerous new questions on the Permian–Triassic boundary (PTB) aftermath. Recent studies have also shown that some nekto-pelagic taxa such as ammonoids and conodonts quickly recovered after the PT crisis, in less than *c*. 1.5 Ma (Orchard 2007; Brayard *et al*. 2009*b*). Indeed, ammonoids were widespread and abundant during the Early Triassic and became one of the dominant clades in the marine biota. Among the four major orders of ammonoids existing during the Permian, only the ceratitids survived the mass extinction (e.g. Brayard *et al*. 2009*b*), and were the root-stock of all Triassic ammonoids as a quasi-monophyletic group (but see Brayard *et al*. 2007*a*; McGowan & Smith 2007). The superfamily Otoceratacea had a short existence during the Griesbachian and is inherited from the Permian. All other Early Triassic ammonoids are generally considered to be derivative from the Xenodiscaceae superfamily (Brayard *et al*. 2006). The ammonoid rediversification was not a gradual process throughout the entire Early Triassic, as it was interrupted by at least two severe diversity drops at the end of the Smithian and of the Spathian. These two extinctions are concomitant with major worldwide events in the geochemical, palynological and sedimentological records, suggesting severe global oceanographic and/or climate shifts during these two intervals, such as anoxia or change in the latitudinal temperature gradient (e.g. Galfetti *et al*. 2007*c*). The end-Smithian extinction was followed by a marked radiation during the Spathian (Fig. 1; see Brayard *et al*. 2006, 2009*a*).

Morphological disparity and taxonomical diversity usually increase jointly during the early history of a clade (Foote 1993), but they do so at various degrees and they can be decoupled in time. Foote (1993) suggested that the discordance between diversity and disparity patterns may be explained not only by artefacts and taxonomical practice, but also by evolutionary processes and special ecological setting. Disparity is thus often assessed to understand how morphological constraints can influence biotic radiations. Combined analyses of morphological disparity and taxonomic diversity thus could provide an enhanced description of macroevolutionary patterns and processes (e.g. Swan & Saunders 1987; Foote 1993; Dommergues *et al*. 1996, 2001; Roy & Foote 1997; McGowan 2004*a*, *b*, 2005; Saunders *et al*. 2004, 2008; Villier & Korn 2004; Navarro *et al*. 2005). A few researchers have previously studied the evolution of ammonoid morphological patterns for the entire Triassic. For instance, using 322 Triassic ammonoid genera (representing 64% of all recognized Triassic genera in 2004), McGowan (2004*a*, *b*, 2005) quantified the morphological evolution of the ammonoid shell during the Triassic using 13 of the 20 characters proposed by Saunders & Swan (1984) on shell coiling, aperture

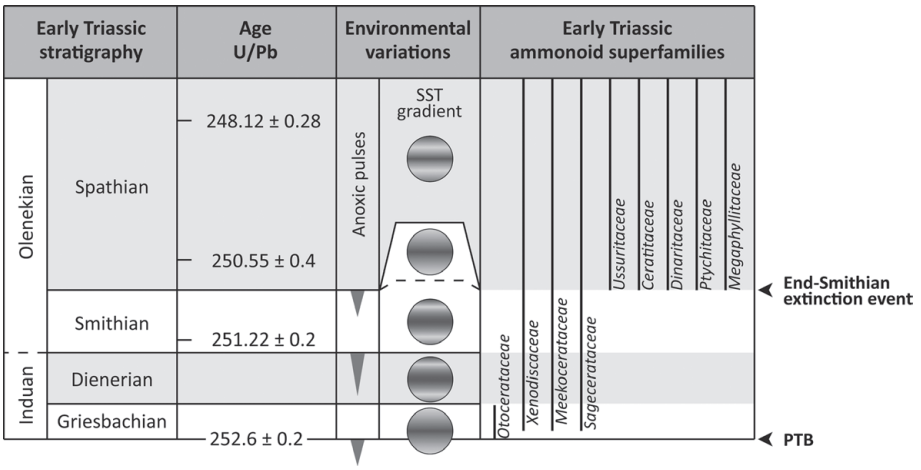

Fig. 1. Simplified Early Triassic chronostratigraphy and potential environmental conditions. Modified from Tozer (1994) and Galfetti *et al*. (2007*a*). Radiometric ages from Mundil *et al*. (2004), Ovtcharova *et al*. (2006) and Galfetti *et al*. (2007*c*). Sea surface temperature (SST) gradient is from Brayard *et al*. (2006, 2007*b*) and possible anoxic pulses from Galfetti *et al*. (2007*a*) and Hermann *et al*. (2011).

shape, ornamentation and suture lines. McGowan (2004*a*, *b*, 2005) noticed that, except for the Dienerian (second substage), the Early Triassic morphological disparity through time was not significantly different from a random pattern. Such a weak signal may be due to the relatively small sample size analysed (e.g. *n* was about 30 for the Dienerian, each specimen representing one genus). However, McGowan (2004*a*, *b*, 2005) identified a decoupling of the taxonomic and morphological signals during the Early Triassic, at least for the Griesbachian (first substage) and the Dienerian, a pattern that is empirically well known by Triassic ammonoid workers. Moreover, as the Dienerian disparity value was low relative to the richness value and concomitant with the absence of sphaeroconic morphotypes, McGowan (2004*a*, *b*) proposed a relationship between the rarity of some morphotypes and contemporaneous palaeoenvironmental settings (e.g. sphaerocone v. anoxia). Villier & Korn (2004) stated that the PTB was marked by the demise of half of the ammonoid superfamilies, and that the Griesbachian disparity pattern was probably strongly biased by a small sample size owing to the paucity of ammonoid-bearing outcrops. Ammonoid disparity evolution during the Early Triassic is here reinvestigated using several recently published data that considerably expand the sample size, and provide complementary and across-scale insights into the ammonoid recovery. The global-scale disparity pattern is compared with five regional signals (e.g. McGowan 2005) of different palaeolatitudes. A potential underlying phylogenetic imprint (at the superfamily level) is also tested. The fluctuations of morphological and phylogenetic diversity patterns are finally compared with previous accounts on taxonomic diversity and discussed according to the events known in the geological record.

Material and methods

Stratigraphy, time scale and main biotic features of the ammonoid recovery

The Early Triassic is officially divided into two substages, the Induan and the Olenekian, defined by Kiparisova & Popov (1956). As the Induan stratotype (located in the Salt Range) is confined to the Tethyan domain and the Siberian Olenekian stratotype is restricted to the Boreal domain, the definition of the Induan–Olenekian boundary is still a matter of debate (see Brühwiler *et al*. 2010*b*, for a recent proposal of Global Stratotype Section and Point (GSSP) candidate in northern India). Moreover, the Induan–Olenekian boundary records a minor ammonoid turnover (Fig. 1) in comparison with other intra-Early Triassic events and still remains poorly defined (see Brühwiler *et al*. 2010*b*). Tozer (1967) established a fourfold subdivision from mid-latitudes of eastern Panthalassa: Griesbachian, Dienerian, Smithian and Spathian (Fig. 1). The subdivisions of Tozer (1967) are relatively well defined in terms of ammonoid and conodont events, and are therefore preferentially used by many Triassic workers and herein. These four subdivisions are now known to be of very uneven durations (Ovtcharova *et al*. 2006; Galfetti *et al*. 2007*b*; Fig. 1). Indeed, the first three substages (Griesbachian, Dienerian and Smithian) have a total duration of less than *c*. 2 Ma, whereas the Spathian (*c*. 3 Ma) lasted more than half the duration of the entire Early Triassic (*c*. 5 Ma; Galfetti *et al*. 2007*b*).

Ammonoid taxonomic and biogeographical patterns drastically changed during the Early Triassic and the rediversification of the clade was not a constant process (e.g. McGowan 2005; Brayard *et al*. 2006, 2007*b*, 2009*a*, *b*). Five main phases can be determined: (1) a low-diversity phase with cosmopolitan assemblages during the Griesbachian; (2) a marked global increase in taxonomic diversity from the Dienerian to the end of the Smithian, with the appearance of a marked latitudinal gradient of diversity and a high endemism; (3) a major extinction during the end-Smithian, which appears to be associated with marked shifts in climate, oceanic circulation and carbon cycle (e.g. Galfetti *et al*. 2007*b*; Brayard *et al*. 2009*b*); (4) a renewed increase in diversity and endemism during the Spathian; (5) another significant drop in diversity at the end of the Early Triassic, near the Spathian–Anisian boundary.

Data

Morphological parameters for 269 Early Triassic ammonoid genera were compiled, representing *c*. 99% of genera known by spring 2011. The first part of the database includes previously or recently published measurements from the early 20th century to the present day. The final dataset covers 30 regions grouped into seven main areas, mainly based on the biogeographical clusters defined by Brayard *et al*. (2007*a*, 2009*a*) (see Fig. 2 and Table 1). These areas are here referred to as: Boreal domain, Equatorial domain, Mid-latitudinal Panthalassa, Tethys–Panthalassa interface, and Southern, Western and Central Tethys. These regions are represented by 3–8 fossiliferous localities. For disparity analyses, the Southern, Central and Western Tethys domains were grouped into a 'Tethyan domain' to cover a longer time-span and to compensate for the poor sampling of the Central Tethys ($n = 30$; see Table 1). As all ammonoid forms occur in most types of facies in the Early Triassic (see Brayard & Escarguel 2012), a preservation bias

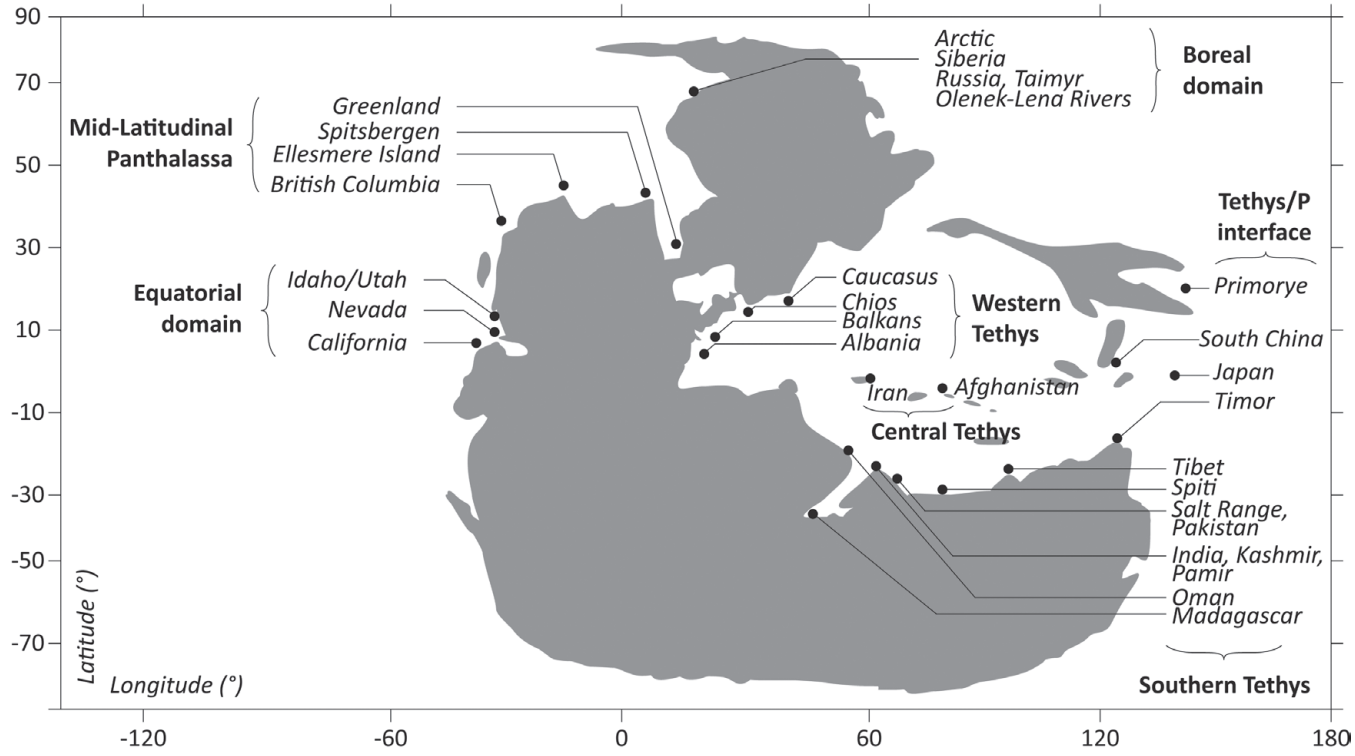

Fig. 2. Early Triassic palaeogeographical map with location of the studied regions. Modified from Brayard *et al*. (2006, 2009*a*).

Table 1. *Distribution of the 30 regions into the seven domains*

	Boreal domain	Mid-latitudinal Panthalassa	Equatorial domain	Tethys–Panthalassa interface	Southern Tethys	Central Tethys	Western Tethys	Tethyan domain
Regions	Arctic, Olenek–Lena Rivers, Russia, Siberia, Taimyr	British Columbia, Ellesmere Island, Greenland, Spitsbergen	California, Idaho, Utah, Nevada	China, Japan, Primorye, Timor	India, Kashmir, Madagascar, Oman, Salt Range, Pakistan, Spiti, Tibet	Afghanistan, Iran, Pamir	Albania, Balkans, Caucasus, Chios	Afghanistan, Albania, Balkans, Caucasus, Chios, India, Iran, Kashmir, Madagascar, Oman, Pakistan, Pamir, Salt Range, Spiti, Tibet
Number of genera	45	57	81	122	96	11	45	152
n	555	265	555	1261	1282	30	641	1953

The Tethyan domain is split into the Southern, Central and Western Tethys basins. *n* represents the sample size (number of measured specimens) for the classical parameter database.

between the various morphologies is probably weak. Moreover, for each region, ammonoid data are pooled from various palaeoenvironments, thus reducing potential facies-related or taphonomic biases in the inter-region comparisons.

The external shell geometry was quantified using a reduced set of variables based on classical and Raup's parameters (Fig. 3). Classical parameters refer to basic shell geometry (conch diameter and relative whorl width, whorl height and umbilical diameter). Raup's parameters refer to the shell coiling geometry (whorl expansion rate, relative aperture height and shape, and relative umbilical diameter (Raup 1966)). Early Triassic genera rarely display marked ornamentation characters and are often represented by the same abundant morphotypes (moderately to strongly evolute compressed conch with coarse and moderately plicate sculpture shell; e.g. III–IV and VIII of Saunders *et al*. 2008). Contrary to some previous studies on ammonoid disparity (e.g. Saunders *et al*. 2004, 2008; McGowan 2004*a*, 2005), no formal attention is paid here to other shell sculptural variables, aperture shape, or suture complexity (e.g. Saunders *et al*. (2004, 2008) used no fewer than 20 parameters). Indeed, following Buckman's laws of covariation (Westermann 1966; Hammer & Bucher 2005*a*; Urdy *et al*. 2010), sculptural variables (such as rib intensity, constriction and strigation) or aperture shape mostly depend on the above-mentioned coiling parameters. The suture line complexity could be useful but it does not seem relevant to our analysis, as suture lines for Early Triassic ammonoid taxa are often similar and the few groups with very distinct suture lines also display specific conch morphologies (e.g. Sageceratacae, Parannanitidae, Ussuriidae). Moreover, the ammonoid shell shows a marked relationship between the expansion of the shell, the external ornamentation, the growth of the soft parts and thus, possibly, the shape of the suture line (e.g. Hammer & Bucher 2005*b*). For example,

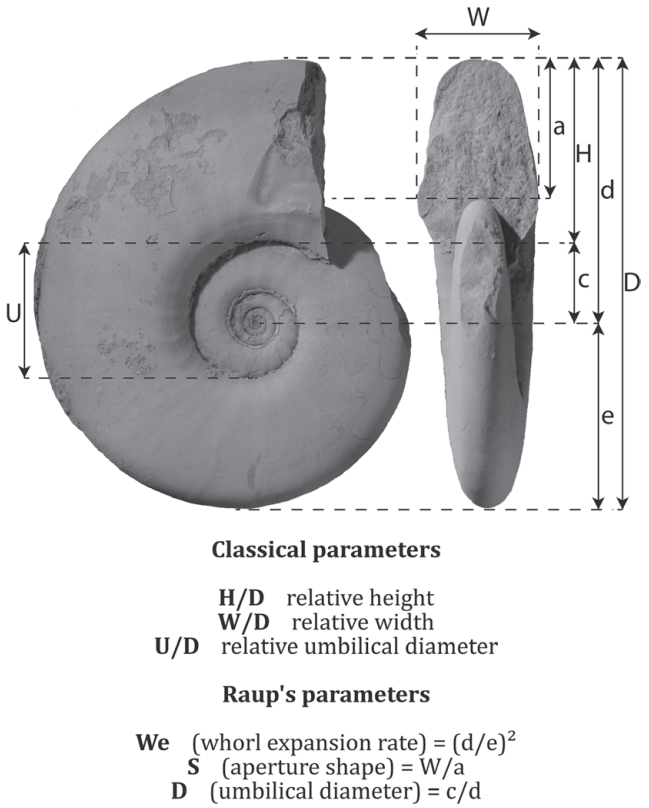

Fig. 3. Morphometric measurements displayed on a Griesbachian (ophiceratid) ammonoid shell.

Monnet *et al*. (2011) documented the covariation between suture line and shell geometry among Devonian pinacitids and auguritids. Lastly, suture lines are often not properly illustrated. The use of a reduced set of variables for the Early Triassic is thus justified and makes our set of morphotypes comparable with those of some previous researchers (e.g. McGowan 2004*a*; Saunders *et al*. 2008). Definition and terminology of ammonoid morphotypes follow Westermann (1996).

Studies on Early Triassic ammonoid morphology are generally performed without much consideration of ontogeny (for a specific exploration in a phylogenetic context, see Korn *et al*. 2003; McGowan & Smith 2007; De Beats *et al*. 2012). To circumvent this problem, disparity analyses generally focus on the adult ammonoid morphology. However, although the characters for recognizing ammonoid adult specimens are well established for several periods (e.g. Devonian; see De Baets *et al*. 2012), mature modifications of the Early Triassic convergent morphs are still poorly documented. Furthermore, they are not always visible on figured specimens. As the recognition of true adult specimens from the Triassic is rather subjective, datasets often record the largest known complete specimen for each genus (e.g. McGowan 2004*a*, 2005; Saunders *et al*. 2008). For instance, Saunders *et al*. (2008) proposed that Palaeozoic ammonoids reached adult morphologies when the shell was 10–25 mm in diameter and presented mature modifications (e.g. ornamentation). Davis *et al*. (1996) specified that the recognition of the adult stage depends on the studied time interval, and was characterized for the Triassic by, for example, changes in body chamber, in whorl section, prominent ornamentation or the fading of sculpture. As juvenile morphologies can markedly differ from the adult morphologies, keeping only the largest specimen probably distorts the main signal. Such a protocol results in an impoverishment of the dataset and, in turn, in a loss of part of the disparity signal. In the present study, the influence of the smallest specimens is studied as a proxy for the influence of juvenile specimens. We seize this opportunity to test whether using only the largest specimens yields patterns similar to those obtained when all specimens or only juvenile specimens are selected.

The main database is composed of 6024 specimens with measured classical parameters. In addition, both classical and Raup's parameters were measured for 1641 other specimens. Individuals with incomplete measures were excluded from the dataset. The final dataset is consequently reduced to 5420 specimens with a complete set of classical parameters, and 972 specimens with a complete set of Raup's parameters (Table 2). As the analyses with both sets of parameters yield very similar results, we present those obtained with the classical parameters only.

Considering that the taxonomy of Early Triassic ammonoids is still continuing, disparity analyses were performed at the genus level, as genus appears to be a more robust taxonomic unit than species. To compare the drastic decrease in generic richness with variations in morphological disparity during the end-Smithian event, the Smithian is therefore subdivided into two distinct time bins: the early–middle Smithian and the late Smithian, as defined by Brühwiler *et al*. (2010*a*). In the Salt Range reference section, the early–middle Smithian corresponds to 12 first ammonoid association zones, from the *Flemingites bhargavai* beds to the *Nyalamites angustecostatus* beds, and the late Smithian corresponds to the two last ammonoid association zones of the Smithian, the *Wasatchites angustecostatus* beds and the *Glyptophiceras sinuatum* beds. A potential underlying phylogenetic imprint is also tested using superfamilies as a proxy. Table 2 summarizes the number of genera obtained for each studied substage of the Early Triassic.

Methods

Principal component analysis (PCA). Ammonoid shell shapes were studied using PCA. In a multidimensional dataset, PCA is used to find a reduced number of hypothetical variables, called principal components, that explain as much variance of the dataset as possible (Gauch 1982; Hammer *et al*. 2004; Saunders *et al*. 2008). The new variables (PCs) are linear combinations of the

Table 2. *Number of specimens and corresponding genera recorded in the global-scale dataset for each studied interval of the Early Triassic*

Griesbachian	Dienerian	Early–middle Smithian	Late Smithian	Spathian	Early Triassic
Classical parameters					
n = 189	*n* = 530	*n* = 2433	*n* = 546	*n* = 1722	*n* = 5420
(19 gen)	(34 gen)	(111 gen)	(12 gen)	(112 gen)	(269 gen)
Raup's parameters					
n = 66	*n* = 62	*n* = 470	*n* = 78	*n* = 296	*n* = 972
(17 gen)	(29 gen)	(98 gen)	(11 gen)	(105 gen)	(239 gen)

The Smithian is divided into early–middle Smithian and late Smithian.

PC	*Eigenvalues*	*%Variance*	*PCA loading*	
1	0.0208	52.5	Umbilical diameter: -0.835	PC1 v. PC2 morphospace: 94% of variance
			Whorl Height: 0.544	
2	0.0166	41.86	Whorl width: 0.995	
3	0.00223	5.63	Whorl Height: -0.8339	
			Umbilical diameter: -0.5491	

Fig. 4. Results of PCA for the global-scale dataset based on classical measurements. PC, principal component. Eigenvalues give a measure of the variance and are used to weight the morphospace axes by their weight within the morphological variability. The percentage of variance represents the weight of each PC in variance. The PCA loading corresponds to the participation of each measured parameter in the ordination of the PCs.

original ones and are independent. This property allows the calculation of disparity parameters. All analyses presented here were performed using the three classical ratio parameters (U/D, H/D, W/D) using Past 2.12 (Hammer *et al*. 2004). Because these variables are ratios with comparable scales, we decided to perform the PCA using the variance/covariance matrices. The data points are then plotted in the coordinate system given by the first two components and express a morphospace.

Sum of variances. Morphological disparity is estimated using scores on the three components of the PCA with the MDA package (Navarro 2003) from the scattering of specimens in a morphospace. It can intuitively be evaluated as the amount of occupied morphospace, but such an approach is sample-dependent: the larger the sample, the more occupied the morphospace (Foote 1993). Another estimator unbiased by sample size is the average distance between points in the morphospace (Van Valen 1974; Foote 1993). Disparity can thus be measured as the sum of variances of all dimensions in a morphospace. Foote (2003) noticed that the disparity and the sum of variance tend to be correlated when using a large sample, which is the case with our dataset. The morphological disparity is consequently displayed as the sum of variances in all our analyses.

Because measured values are sample-dependent and prone to different biases, a standard error is computed with a bootstrap procedure with a 95% confidence interval. The standard deviation tends to be stable with a minimal value of 200 bootstrap iterations (Navarro 2003), but most studies used 500–1000 iterations. The great amount of data for the global-scale dataset constrains the bootstrap resampling used in this study to a maximum of 200 iterations for the global-scale analyses and 500 iterations for the regional-scale analyses.

Putative sampling biases have not been corrected by any rarefaction techniques. As presented in Table 2, sample size varies from n = 189 for the Griesbachian to n = 2433 for the early–middle Smithian. A standardization of sample size to the smallest sample would require keeping only 189 out of 2433 samples for the early–middle Smithian. Rarefaction would considerably reduce the dataset and is therefore not used in this study. Furthermore, we suspect these differences in sample size to reflect the Griesbachian to Smithian ammonoid radiation rather than only a heterogeneously sampled fossil record.

Results

Global patterns of morphological disparity

The PC1 v. PC2 morphospace represents 94% of the variance (respectively 52.50 and 41.86%; Fig. 4) for the dataset based on classical parameters. The two first components are mostly defined by the relative umbilical diameter and whorl width (or by aperture shape and whorl expansion rate in the case of Raup's parameters). The obtained 2D morphospace thus characterizes the tightness of coiling (involution) and the whorl section compression of the ammonoid shells. The high value of 94% of variance explained by the PC1 v. PC2 morphospace permits to keep a simple two-dimensional iconography to illustrate the evolution of variances (Fig. 5a). The morphospace occupation has a triangular shape during the Early Triassic, the angles of which broadly correspond to involute compressed, evolute compressed and depressed shells (respectively corresponding to the extreme oxyconic (e.g. *Hedenstroemia, Pseudosageceras, Aspenites*), serpenticonic (e.g. *Dieneroceras, Xenoceltites*) and sphaeroconic (e.g. *Paranannites, Juvenites*) morphotypes). The borders of the occupied morphospace probably reflect the limiting role of geometrical constraints on the shell coiling (e.g. Raup 1967). Figure 5b and c compares the evolution of disparity with generic richness through the Early Triassic. Although the two curves do not perfectly match, they both reach a maximum value during the early–middle Smithian and a second peak during the Spathian. The two peaks are separated by low values corresponding to the marked extinction event of the end-Smithian. The main difference between the two curves occurs during the Griesbachian, for which the generic richness is very low whereas morphological disparity is relatively high. This mismatch lasted until the Dienerian, when the generic richness shows a weak increase and the disparity becomes minimal. During the Spathian, a third mismatch is visible, as the generic richness reaches the same value as during the early–middle Smithian whereas the disparity shows a relatively lower value. This result has to be interpreted with caution, however. Indeed, several taxonomic studies on this substage are still in preparation and they will probably increase the generic richness of this interval significantly without greatly affecting its disparity.

Regional patterns of morphological disparity

A similar evolution of disparity is observed between the global-scale curve and all regional curves, with low values characterizing the Dienerian and the late Smithian (Fig. 6). The high early–middle Smithian disparity is also recorded in all cases. Such analogous patterns suggest common abiotic global processes. The Equatorial domain is an exception to this pattern, as the corresponding level of disparity is restricted during the Spathian. This may result from the endemism of most Spathian taxa reported from this area and the fact that they often have similar shell morphologies. Griesbachian and Dienerian patterns are not known from this domain owing to the rarity of ammonoid occurrences from these two substages. The recently published Dienerian ammonoid assemblage from the Candelaria Formation of western USA by Ware *et al*. (2011) was not included in this work, but is unlikely to change significantly the observed disparity pattern.

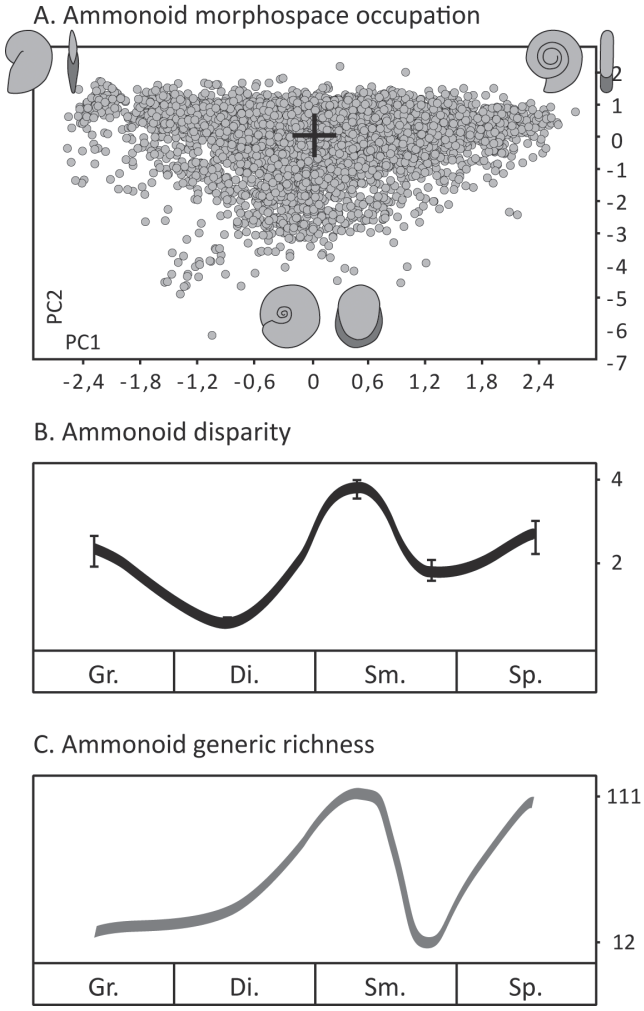

Fig. 5. (**a**) PC1 v. PC2 morphospace occupation during the entire Early Triassic. (**b**, **c**) Disparity and generic richness through the Early Triassic. Both curves are based on classical parameters. The length of each subdivision is not proportional to absolute time durations. Gr, Griesbachian; Di, Dienerian; Sm, Smithian; Sp, Spathian.

Influence of juvenile specimens on morphospace occupation

Figure 7a illustrates the sum of variances throughout the Early Triassic, when only the specimen with the smallest diameter of each genus is considered (the resulting dataset is called Dmin). The curve depicting the fluctuation of disparity is very similar to the one based on the complete dataset (Fig. 5b). Figure 7b displays the scatter-plots of the smallest specimens (diameter <15 mm) within the morphospace. These specimens are not clustered in a particular area and rarely occupy the periphery of the morphological landscape. This is also true when the third dimension of the morphospace is included.

As (1) the smallest specimens do not seem to modify the patterns obtained with the complete dataset, (2) the morphological signal of smallest specimens is part of the global pattern, and (3) the recognition of true adult individuals is still a matter of debate and some ammonoids might reach maturity at very small sizes, small specimens were kept in all subsequent analyses.

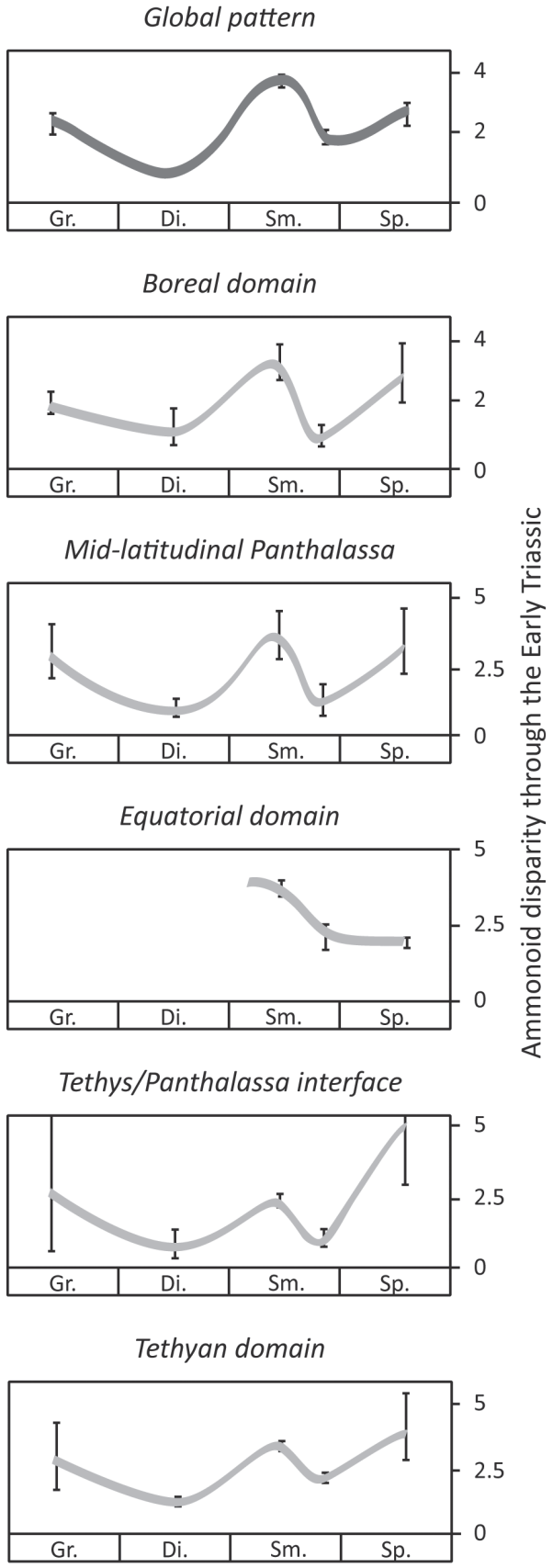

Fig. 6. Evolution of ammonoid disparity through the Early Triassic for the five studied domains. Abbreviations as in Figure 5.

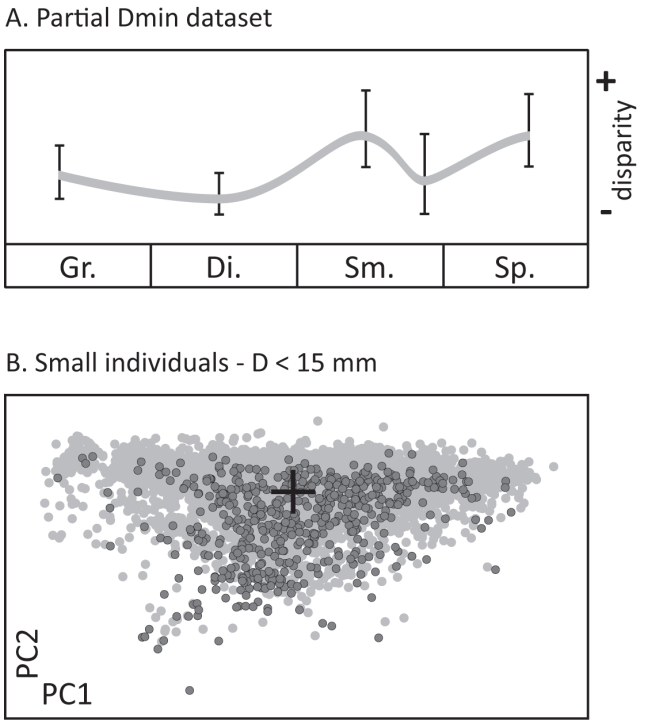

Fig. 7. (**a**) Disparity through time based on the partial Dmin dataset built with the smallest specimen of each genus (n = 269). (**b**) PC1 v. PC2 morphospace highlighting the individuals smaller than 15 mm (dark dots) within the complete dataset. Abbreviations as in Figure 5.

Evolution of morphospace occupation

Figure 8 shows the morphospace occupation for each studied Early Triassic interval. The decreases in disparity during the Dienerian and the late Smithian do not correspond to a homogeneous contraction of the morphospace. They mostly correspond to restricted losses on the peripheral edges of the morphospace that lead to the disappearance of extreme morphotypes. The following patterns were documented.

(1) During the Griesbachian, three extreme morphotypes occur: oxyconic forms (left part of the morphospace), serpenticonic forms (right part) and rare sphaeroconic forms (lower part).
(2) A marked contraction and shift of the morphospace toward the most closely coiled (involute) pole is observed during the Dienerian, with the loss of the most evolute forms and the appearance of new involute forms.
(3) The early–middle Smithian ammonoids then occupy every part of the wide Early Triassic morphological landscape. Several globular forms appear.
(4) The morphospace is again reduced during the late Smithian with the loss of extreme evolute and globular morphologies. Moreover, the scatter-plot is divided into two groups, corresponding to two main superfamilies (see discussion below).
(5) The Spathian morphospace is analogous to the early–middle Smithian morphospace, with the reappearance of several globular forms. Surprisingly, sphaerocones are the most commonly affected during the Dienerian and end-Smithian extinction.

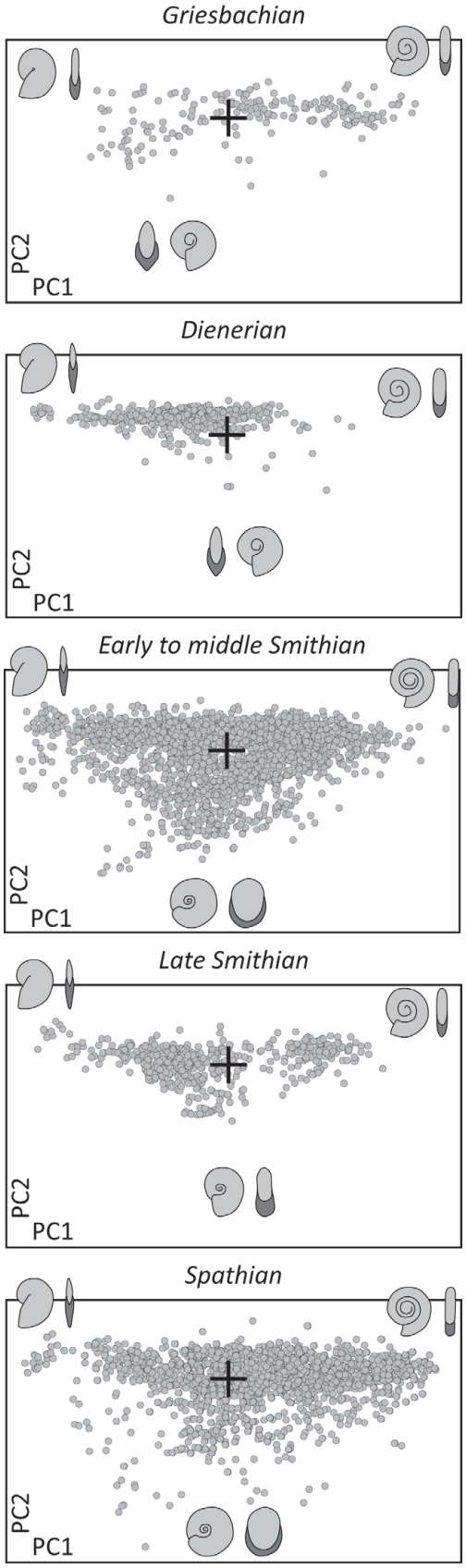

Fig. 8. PC1 v. PC2 morphospace occupation by ammonoids during each studied Early Triassic interval. Extreme morphotypes are illustrated at the morphospace poles.

The contributions of superfamilies

Early Triassic ammonoids belong to *c*. 50 families grouped into nine superfamilies. These superfamilies follow the classification of Tozer (1967) and are consensually regarded as being monophyletic. Consequently, we consider the patterns described here as robust in spite of some expected taxonomic changes owing to the large number of new taxa described recently (e.g. Brühwiler *et al*. 2012). Only three superfamilies ranged through the entire Early Triassic: Meekoceratoceae, Xenodiscaceae and Sageceratoceae (Fig. 1). Figure 9a displays the evolution in morphospace occupation for each of these superfamilies and Figure 9b illustrates their respective contribution to the total disparity. Complete morphological data are missing for the Griesbachian Sageceratoceae, but this superfamily did occur within this substage (see, e.g. Brayard *et al*. 2006, 2009*a*; Brühwiler *et al*. 2010*b*). The Otoceratoceae (pale grey dots in Fig. 9a; Griesbachian) form a clade probably inherited from the Permian, which disappeared rapidly after the PT crisis. This superfamily is responsible for *c*. 25% of the total Griesbachian disparity (Fig. 9). Their disappearance leads to the impoverishment of the oxycone pole during the Dienerian. The serpenticone pole is also reduced during the Dienerian by the decline of Xenodiscaceae. The morphospace is widely colonized during the early–middle Smithian with the additional appearance of sphaeroconic morphotypes. The late Smithian event restricts the morphospace of each superfamily. At the same time, the disappearance of the sphaeroconic shells coincides with the extinction of the Melagathiceratidae and of the Paranannitidae (belonging to the Xenodiscaceae and Meekoceratoceae superfamilies respectively). Five new superfamilies diversified and eight coexisted during the Spathian (details not given in Fig. 9a; Spathian, pale grey dots). The relative contribution of these new superfamilies is displayed in Figure 9b. Despite the PC1 v. PC2 morphospaces being notably similar between the early–middle Smithian and the Spathian, *c*. 70% of the Spathian morphospace results from the appearance of these five new superfamilies. The three oldest superfamilies occurring during the Griesbachian, Dienerian and Smithian (Xenodiscaceae, Meekoceratoceae and Sageceratoceae) thus do not show a marked morphological diversification at that time.

Discussion

Taxonomic richness v. disparity

Global patterns. As simplified in Figure 10, the patterns of disparity discussed herein clearly show significant Early Triassic fluctuations that were partly decoupled from changes in generic richness, especially during the Griesbachian–Dienerian and the end-Smithian intervals. This differs from previous results (e.g. McGowan 2004*a*, 2005). On the one hand, the exceptionally low disparity during the Dienerian, previously reported by McGowan (2004*a*), could here be identified as a robust pattern by increasing the sampling size. On the other hand, the marked impact of the late Smithian extinction on ammonoid disparity is reported for the first time. Foote (1993) defined six idealized cases of qualitative differential evolution between disparity and generic richness (Fig. 11). Although Foote's (1993) cases were not specifically defined for mass extinction recovery, three of them may correspond to our results. Villier & Korn (2004) and Saunders *et al*. (2008) suggested that the earliest Triassic morphospace occupation was restricted and similar to the Late Permian one. Although their studies involved a very small number of Griesbachian specimens (e.g. $n = 11$ in the study by Saunders *et al*. 2008), our results are consistent with the previous observations of a very low diversity and high disparity during the Griesbachian (Fig. 10). According to Foote (1993), such a pattern may be diagnostic of a nonselective extinction, randomly affecting the morphospace landscape without generating a severe contraction (Fig. 11). Villier & Korn (2004) interpreted this pattern as characteristic of a 'mass-extinction regime', which may be due to global severe environmental variations affecting most ecological niches. The Dienerian increase in generic richness is concomitant with a low disparity level, characterized by the disappearance of the serpenticonic and sphaeroconic shells. Foote (1993) referred to such a decoupling as a morphologically constrained radiation (Fig. 11) owing to ecological selectivity. The morphospace is then widely enlarged by a colonization of the (sub)globular pole of the morphological landscape during the early–middle Smithian (Fig. 9a). In that case, the taxonomical diversification also corresponds to a morphological expansion. The late Smithian extinction mainly affected the sphaeroconic morphotype (case 3 in Fig. 11: no major constraint in the morphological evolution). It is now well known that this biotic event corresponds to contemporaneous changes in the sedimentological, geochemical and palynological records suggesting changes in the global climate and in the redox state of oceanic waters (e.g. Galfetti *et al*. 2007*a*, *b*, *c*; Hermann *et al*. 2011). The Spathian rediversification resulted from the appearance of five new superfamilies. In spite of a greater number of superfamilies and a broader range of ornamentation and suture lines, the morphospace occupation is similar to that of the Smithian. Griesbachian to early–middle Smithian dominant superfamilies (Meekoceratoceae, Sageceracateae and Xenodiscaceae) did not regain their initial high level of disparity (Fig. 9). They were replaced by newcomers occupying more restricted parts of morphospace. The presence of extreme forms is also in agreement with biogeographical analyses indicating a high proportion of endemic ammonoid taxa during the Spathian (e.g. Brayard *et al*. 2006).

Regional patterns. Similar fluctuations in global and regional disparity patterns during the Early Triassic (Fig. 6) suggest that regional patterns do not result from a single over-sampled province. Moreover, they indicate that the recovery in morphological disparity was simultaneous within all provinces, at least until the Spathian.

A superfamily imprint on disparity?

Although the morphospace was severely reduced during the late Smithian extinction, the ammonoids involved in the Spathian radiation occupied the morphospace in a similar way to the early–middle Smithian taxa (Fig. 9). The Spathian morphospace resulted from the appearance of five new superfamilies colonizing empty parts of the morphospace (e.g. globular forms), and boundary-crossing superfamilies did not reach the same disparity levels as in the Smithian again. One working hypothesis is that Spathian superfamilies occupied more restricted ecological niches than before. The globular morphotype area was filled by different superfamilies (mainly Meekoceratoceae, Ceratitaceae and Dinaritaceae). Therefore, based on the hypothesis of a relationship between ammonoid shell geometry and habitat (e.g. Westermann 1971, 1996; Wang & Westermann 1993; Saunders *et al*. 2008; Monnet *et al*. 2011), this suggests that phylogenetically distant taxa may have occupied similar ecological niches and that the iterative ability to evolve this morphotype was common among their

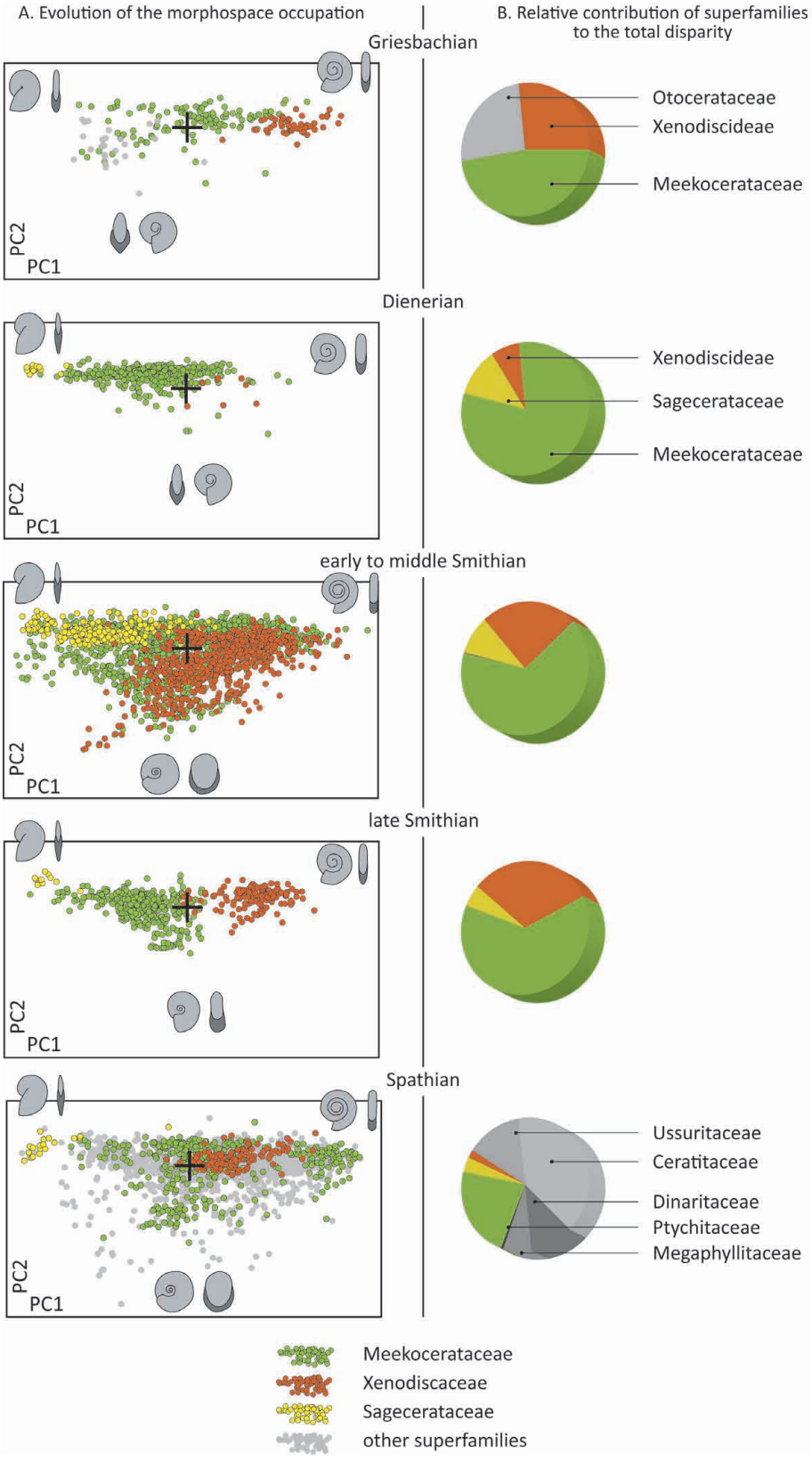

Fig. 9. (**a**) Evolution of the PC1 v. PC2 morphospace during the Early Triassic, with the three main superfamilies highlighted. (**b**) Relative contribution of the Early Triassic superfamilies to total disparity.

lineages. A comparable case may be found for some Jurassic ammonoids, where one clade (the Hammatoceratidae) tends to colonize during its history a part of the morphospace previously occupied by some other groups, these later being then morphologically more restricted (Neige *et al*. 2001). Another potential process for explaining the morphospace recolonization is a simple unconstrained diffusion of the

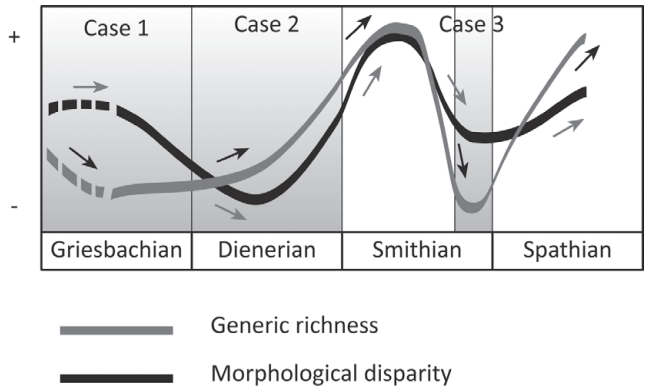

Fig. 10. Superimposition of generic richness and disparity curves for the Early Triassic ammonoids. Correspondence to three of the macroevolutionary cases of Foote (1993) is highlighted.

Spathian superfamilies towards the sphaeroconic pole, after being reduced in richness and disparity during the end-Smithian crisis.

Potential environmental parameters influencing disparity

Figure 1 displays inferred climatic variations for each studied Early Triassic interval based on different proxies. Morphospace occupation and evolution potentially reflect environmental influences such as climatic variations. This appears to be the case for the late Smithian extinction when the ammonoid morphological landscape was severely reduced with the complete disappearance of most sphaeroconic taxa (lower pole of the morphospace), both in Meekoceratoceae and Xenodiscaceae (Fig. 9). Therefore, the restricted morphospace occupation was not the consequence of the exclusive disappearance of a single superfamily. It thus cannot be mainly attributed to a phylogenetically driven process. As the late Smithian extinction is probably linked to a contemporaneous global climatic change (e.g. Brayard *et al*. 2006, 2009*a*; Galfetti *et al*. 2007*a*, *c*; Hermann *et al*. 2011), both diversity and disparity drops have possibly been triggered by this global event.

During the Dienerian, disparity is very low because the sphaeroconic and serpenticonic morphotypes are largely absent. In contrast to the late Smithian, the contraction of the Dienerian morphospace cannot be unambiguously related to a climatic phenomenon although this substage probably corresponds to a relatively weak latitudinal sea surface temperature gradient (Brayard *et al*. 2006, 2007*b*, 2009*a*). The restricted disparity during the Dienerian substage and the late Smithian event might also be concomitant with recurrent fluctuations of other major environmental parameters such as anoxia. In support of this hypothesis, Hermann *et al*. (2011) reported disoxic conditions during the Dienerian in Pakistan, coeval with disoxic or anoxic marine sediments of South China and North India (Galfetti *et al*. 2007*a*) and possibly in Nevada (Ware *et al*. 2011). The end-Smithian event seems also to be associated with some anoxic deposits within restricted but distant areas such as the northern Gondwana margin and the South China Block (Galfetti *et al*. 2007*b*; Hermann *et al*. 2011). On the one hand, following this hypothesis, such harsh environmental conditions could have induced a worldwide selection against the sphaeroconic morphotype. However, it appears surprising that this morphotype did not escape these environmental changes. Various relationships between ammonoid morphologies and particular lifestyles have also been hypothesized (e.g. Raup & Chamberlain 1967; Swan & Saunders 1987; Jacobs 1992; Batt 1993; Wang & Westermann 1993; Jacobs *et al*. 1994; Westermann 1996; Klug & Korn 2004; Monnet *et al*. 2011) although it clearly remains speculative to attribute a specific ecological niche to a given morphotype. Sphaeroconic morphotypes were, for instance, interpreted as inhabitants of low-energy offshore environments by Jacobs (1992) and Jacobs *et al*. (1994), as vertical migrants by Westermann (1996) and as slow demersal swimmers by Swan & Saunders (1987). The globular forms are therefore generally assumed to be less adapted to shallow high-energy environments. On the other hand, as the sphaeroconic morphotype episodically reappeared several times during the Early Triassic, this might be simply explained by a relaxing of ecological constraints, allowing the occupation of previously empty ecological niches. The morphospace could also be refilled by convergent evolution (e.g. Monnet *et al*. 2011) in the various regions or by rapid dispersal (e.g. De Baets *et al*. 2012).

Conclusion

The use of a reduced set of classical conch parameters appears appropriate for investigating the morphological evolution of Early Triassic ammonoids, as they permit simple analytical procedures and the use of large datasets. Considering previous results obtained by Swan & Saunders (1987), Saunders *et al*. (2004, 2008) and Villier & Korn (2004) on Middle–Late Permian ammonoids that appear similar to the Early Triassic morphospace, we hypothesize that this procedure is pertinent for future analyses on the rest of the Triassic, which presents the same set of very abundant morphotypes (III–IV and VIII of Saunders *et al*. 2008).

Similarly to the taxonomic rediversification, the morphological recovery appears to have quickly reached high values during the Early–Middle Smithian, which is consistent with previous studies by Brayard *et al*. (2006, 2009) indicating that the ammonoid taxonomic recovery was rapid: it lasted less than *c*. 1.5 Ma.

	Generic richness	*Disparity*	*Causes*
Case 1	↘	→	Random distribution of extinction in the morphospace
Case 2	↗	→	Highly morphologically constrained radiation
Case 3	↘	↘	Extinction of extreme morphotypes
Case 4	→	→	No major constraint in the morphological evolution
Case 5	↘	→	Selective extinction of modal forms.
Case 6	↘	↗	Adaptative radiation leading to wide exploration of morphospace

Fig. 11. Six idealized evolutionary possibilities of ammonoid rediversification, after Foote (1993). The shaded rows correspond to the three processes that can be identified for this study. Arrows indicate stability of, increase of, or decrease in generic richness or in disparity.

The comparison of global versus regional signals showed that the Early Triassic morphological recovery was simultaneous and parallel in all palaeobiogeographical areas studied here, with the exception of the equatorial domain, the signal for which is due to the scarcity of ammonoid data during the Griesbachian and Dienerian, and probably to the high endemism of the Spathian ammonoids. The decoupling between diversity and disparity is probably characteristic of a nonselective extinction at the PTB, a constrained radiation during the Dienerian and a possibly deterministic extinction (following the nomenclature of Foote 1993) at the Smithian–Spathian boundary. The high disparity value observed during the Spathian can be explained by the diversification of five new superfamilies within restricted portions of the morphospace or by an unconstrained recolonization of the Spathian superfamilies towards the sphaeroconic pole, after being reduced in richness and disparity during the end-Smithian crisis. Morphological disparity evolution may have been constrained by environmental changes (e.g. during the Dienerian interval) rather than by the taxonomic richness. Indeed, sphaeroconic ammonoids appear to be the most affected morphotype when harsh ecological conditions such as extreme climate or widespread anoxia prevailed. However, as the sphaeroconic morphotype occurred episodically during the Early Triassic, this might be simply explained by a relaxing of ecological constraints, allowing the occupation of previously empty ecological niches, or by morphospace refilling by convergent evolution in various regions.

This paper is a contribution to the team BioME of the UMR CNRS 6282 and was funded by the Région Bourgogne, the FRB, and the CNRS INSU Interrvie. J. Neenan (Zurich) improved the English text. T. Brühwiler and D. Ware (Zurich) kindly shared some of their unpublished measurements. C. Monnet (Lille) and two anonymous reviewers provided constructive reviews, which helped us to improve the paper.

References

Batt, R. 1993. Ammonite morphotypes as indicators of oxygenation in a Cretaceous epicontinental sea. *Lethaia*, **26**, 49–63, doi:10.1111/j.1502-3931.1993.tb01511.x.

Brayard, A. & Escarguel, G. 2012. Untangling phylogenetic, geometric and ornamental imprints on Early Triassic ammonoid biogeography: A similarity–distance decay study. *Lethaia*, **46**, 19–33, doi:10.1111/j.1502–3931.2012.00317.x.

Brayard, A., Bucher, H., Escarguel, G., Fluteau, F., Bourquin, S. & Galfetti, T. 2006. The Early Triassic ammonoid recovery: paleoclimatic significance of diversity gradients. *Palaeogeography, Palaeoclimatology, Palaeoecology*, **239**, 374–395, doi:10.1016/j.palaeo.2006.02.003.

Brayard, A., Bucher, H., *et al*. 2007*a*. *Proharpoceras* Chao: A new ammonoid lineage surviving the end-Permian mass extinction. *Lethaia*, **40**, 175–181, doi:10.1111/j.1502-3931.2007.00012.x.

Brayard, A., Escarguel, G. & Bucher, H. 2007*b*. The biogeography of Early Triassic ammonoid faunas. Clusters, gradients, and networks. *Geobios*, **40**, 749–765, doi:10.1016/j.geobios.2007.06.002.

Brayard, A., Escarguel, G., Bucher, H. & Brühwiler, T. 2009*a*. Smithian and Spathian (Early Triassic) ammonoid assemblages from terranes: paleoceanographic and paleogeographic implications. *Journal of Asian Earth Sciences*, **36**, 420–433, doi:10.1016/j.jseaes.2008.05.004.

Brayard, A., Escarguel, G., *et al*. 2009*b*. Good genes and good luck. Ammonoid diversity and the end-Permian mass extinction. *Science*, **325**, 1118–1121, doi:10.1126/science.1174638.

Brayard, A., Vennin, E., *et al*. 2011. Transient metazoan reefs in the aftermath of the end-Permian mass extinction. *Nature Geoscience*, **4**, 693–697, doi:10.1038/ngeo1264.

Brühwiler, T., Bucher, H., Brayard, A. & Goudemand, N. 2010*a*. High-resolution biochronology and diversity dynamics of the Early Triassic ammonoid recovery: The Smithian faunas of the Northern Indian Margin. *Palaeogeography, Palaeoclimatology, Palaeoecology*, **297**, 491–501, doi:10.1016/j.palaeo.2010.09.001.

Brühwiler, T., Bucher, H. & Goudemand, N. 2010*b*. Smithian (Early Triassic) ammonoids from Tulong, South Tibet. *Geobios*, **43**, 403–431, doi:10.1016/j.geobios.2009.12.004.

Brühwiler, T., Bucher, H., Goudemand, N. & Galfetti, T. 2012. Smithian (Early Triassic) ammonoid faunas from exotic blocks from Oman: Taxonomy and biochronology. *Palaeontographica, Abteilung A*, **296**, 3–107.

Davis, R.A., Landman, N.H., Dommergues, J.-L., Marchand, D. & Bucher, H. 1996. Mature modifications and dimorphism in Ammonoid cephalopods. *Ammonoid Paleobiology*, **13**, 464–539.

De Baets, K., Klug, C., Korn, D. & Landman, N.H. 2012. Early evolutionary trends in ammonoid embryonic development. *Evolution*, **66**, 1788–1806, doi:10.1111/j.1558-5646.2011.01567.x.

Dommergues, J.L., Laurin, B. & Meister, C. 1996. Evolution of ammonoid morphospace during the Early Jurassic radiation. *Paleobiology*, **22**, 219–240, doi:10.2307/2401118.

Dommergues, J.L., Laurin, B. & Meister, C. 2001. The recovery and radiation of Early Jurassic ammonoids: Morphologic versus palaeobiogeographical patterns. *Palaeogeography, Palaeoclimatology, Palaeoecology*, **165**, 195–213, doi:10.1016/S0031-0182(00)00160-7.

Erwin, D.H. 2001. Lessons from the past: Biotic recoveries from mass extinctions. *Proceedings of the National Academy of Sciences of the USA*, **98**, 5399–5403, doi:10.1073/pnas.091092698.

Foote, M. 1993. Discordance and concordance between morphological and taxonomic diversity. *Paleobiology*, **19**, 185–204, doi:10.2307/2400876.

Foote, M. 2003. Origination and extinction through the Phanerozoic: a new approach. *Journal of Geology*, **111**, 125–148, doi:10.1086/345841.

Galfetti, T., Bucher, H., *et al*. 2007*a*. Late Early Triassic climate change: Insights from carbonate carbon isotopes, sedimentary evolution and ammonoid paleobiogeography. *Palaeogeography, Palaeoclimatology, Palaeoecology*, **243**, 394–411, doi:10.1016/j.palaeo.2006.08.014.

Galfetti, T., Bucher, H., *et al*. 2007*b*. Timing of the Early Triassic carbon cycle perturbations inferred from new U–Pb ages and ammonoid biochronozones. *Earth and Planetary Science Letters*, **258**, 593–604, doi:10.1016/j.epsl.2007.04.023.

Galfetti, T., Hochuli, P.A., Brayard, A., Bucher, H., Weissert, H. & Vigran, J.O. 2007*c*. Smithian–Spathian boundary event: evidence for global climatic change in the wake of the end-Permian biotic crisis. *Geology*, **35**, 291–294, doi:10.1130/G23117A.1.

Gauch, H.G. 1982. Noise-reduction by eigenvector ordinations. *Ecology*, **63**, 1643–1649, doi:10.2307/1940105.

Hammer, Ø. & Bucher, H. 2005*a*. Buckman's first law of covariation—a case of proportionality. *Lethaia*, **38**, 67–72, doi:10.1080/00241160510013196.

Hammer, Ø. & Bucher, H. 2005*b*. Models for the morphogenesis of the molluscan shell. *Lethaia*, **38**, 111–122, doi:10.1080/00241160510013222.

Hammer, Ø., Harper, D.A.T. & Ryan, P.D. 2004. Past: paleontological statistics software package for education and data analysis. *Palaeontologia Electronica*, **4**, 31, doi:10.1080/00241160510013222.

Hermann, E., Hochuli, P.A., *et al*. 2011. Organic matter and palaeoenvironmental signals during the Early Triassic biotic recovery: The Salt Range and Surghar Range records. *Sedimentary Geology*, **234**, 19–41, doi:10.1016/j.sedgeo.2010.11.003.

Hofmann, R., Goudemand, N., Wasmer, M., Bucher, H. & Hautmann, M. 2011. New trace fossil evidence for an early recovery signal in the aftermath of the end-Permian mass extinction. *Palaeogeography, Palaeoclimatology, Palaeoecology*, **310**, 216–226, doi:10.1016/j.palaeo.2011.07.014.

Jacobs, D.K. 1992. Shape, drag, and power in ammonoid swimming. *Paleobiology*, **18**, 203–220.

Jacobs, D.K., Landman, N.H.Y. & Chamberlain, J.A. 1994. Ammonite shell shape covaries with facies and hydrodynamics—Iterative evolution as a response to changes in basinal environment. *Geology*, **22**, 905–908, doi:10.2307/2400999.

Kiparisova, L.D. & Popov, I.N. 1956. Subdivision of the lower series of the Triassic System into stages. *Doklady Akademii Nauk SSSR*, **109**, 842–845.

Klug, C. & Korn, D. 2004. The origin of ammonoid locomotion. *Acta Palaeontologica Polonica*, **49**, 235–242.

Korn, D., Ebbighausen, V., Bockwinkel, J. & Klug, C. 2003. The A-mode sutural ontogeny in prolecanitid ammonoids. *Palaeontology*, **46**, 1123–1132, doi:10.1046/j.0031-0239.2003.00336.x.

McGowan, A.J. 2004*a*. Ammonoid taxonomic and morphologic recovery patterns after the Permian–Triassic. *Geology*, **32**, 665–668, doi:10.1130/G20462.1.

McGowan, A.J. 2004*b*. The effect of the Permo-Triassic bottleneck on Triassic ammonoid morphological evolution. *Paleobiology*, **30**, 369–395, doi:10.1666/;0094–8373.

McGowan, A.J. 2005. Ammonoid recovery from the Late Permian mass extinction event. *Comptes Rendus Palevol*, **4**, 517–530, doi:10.1016/j.crpv.2005.02.004.

McGowan, A.J. & Smith, A.B. 2007. Ammonoids across the Permian/Triassic boundary: A cladistic perspective. *Palaeontology*, **50**, 573–590, doi:10.1111/j.1475-4983.2007.00653.x.

Monnet, C., De Baets, K. & Klug, C. 2011. Parallel evolution controlled by adaptation and covariation in ammonoid cephalopods. *BMC Evolutionary Biology*, **11**, 115, doi:10.1186/1471-2148-11-115.

MUNDIL, R., LUDWIG, K.R., METCALFE, I. & RENNE, P.R. 2004. Age and timing of the Permian mass extinctions: U/Pb dating of closed-system zircons. *Science*, **305**, 1760–1763, doi:10.1126/science.1101012.

NAVARRO, N. 2003. MDA: A MATLAB-based program for morphospace–disparity analysis. *Computers and Geosciences*, **29**, 655–664, doi:10.1016/S0098-3004(03)00043-8.

NAVARRO, N., NEIGE, P. & MARCHAND, D. 2005. Faunal invasions as a source of morphological constraints and innovations? The diversification of the early Cardioceratidae (Ammonoidea; Middle Jurassic). *Paleobiology*, **35**, 98–116, doi:10.1016/S0098-3004(03)00043-8.

NEIGE, P., ELMI, S. & RULLEAU, L. 2001. Existe-t-il une crise au passage Lias–Dogger chez les ammonites? Approche morphométrique par quantification de la disparité morphologique. *Bulletin de la Société Géologique de France*, **172**, 125–132, doi:10.2113/172.2.257.

ORCHARD, M.J. 2007. Conodont diversity and evolution through the latest Permian and Early Triassic upheavals. *Palaeogeography, Palaeoclimatology, Palaeoecology*. **252**, 93–117, doi:10.1016/j.palaeo.2006.11.037.

OVTCHAROVA, M., BUCHER, H., SCHALTEGGER, U., GALFETTI, T., BRAYARD, A. & GUEX, J. 2006. New Early to Middle Triassic U–Pb ages from South China: calibration with ammonoid biochronozones and implications for the timing of the Triassic biotic recovery. *Earth and Planetary Science Letters*, **243**, 463–475, doi:10.1016/j.epsl.2006.01.042.

RAUP, D.M. 1966. Geometric analysis of shell coiling: general problems. *Journal of Paleontology*, **40**, 1178–1190.

RAUP, D.M. 1967. Geometric analysis of shell coiling: coiling in ammonoids. *Journal of Paleontology*, **41**, 43–65.

RAUP, D.M. 1979. Size of the Permo-Triassic bottleneck and its evolutionary implications. *Science*, **206**, 217–218, doi:10.1126/science.206.4415.217.

RAUP, D.M. & CHAMBERLAIN, J.A. 1967. Equations for volume and center of gravity in ammonoid shells. *Journal of Paleontology*, **41**, 566–574.

RODLAND, D.L. & BOTTJER, D.J. 2001. Biotic recovery from the end-Permian mass extinction: Behavior of the inarticulate brachiopod *Lingula* as a disaster taxon. *Palaios*, **16**, 95–101, doi:10.1669/;0883–1351.

ROY, K. & FOOTE, M. 1997. Morphological approaches to measuring biodiversity. *Trends in Ecology & Evolution*, **12**, 277, doi:10.1016/S0169-5347(97)81026-9.

SAUNDERS, W.B. & SWAN, A.R.H. 1984. Morphology and morphologic diversity of Mid-Carboniferous (Namurian) ammonoids in time and space. *Paleobiology*, **10**, 195–228.

SAUNDERS, W.B., WORK, D.M. & NIKOLAEVA, S.V. 2004. The evolutionary history of shell geometry in Paleozoic ammonoids. *Paleobiology*, **30**, 19–43, doi:10.1666/07053.1.

SAUNDERS, W.B., GREENFEST-ALLEN, E., WORK, D.M. & NIKOLAEVA, S.V. 2008. Morphologic and taxonomic history of Paleozoic ammonoids in time and morphospace. *Paleobiology*, **34**, 128–154, doi:10.1666/07053.1.

SCHUBERT, J.K. & BOTTJER, D.J. 1992. Early Triassic stromatolites as post mass extinction disaster forms. *Geology*, **20**, 883–886, doi:10.1130/;0091-7613.

SONG, H.J., WIGNALL, P.B., *ET AL.* 2011. Recovery tempo and pattern of marine ecosystems after the end-Permian mass extinction. *Geology*, **39**, 739–742, doi:10.1130/G32191.1.

SWAN, A.R.H. & SAUNDERS, W.B. 1987. Function and shape in late Paleozoic (mid-Carboniferous) ammonoids. *Paleobiology*, **13**, 297–311.

TOZER, E.T. 1967. *A standard for Triassic time*. Geological Survey of Canada, Bulletin, **156**.

TOZER, E.T. 1994. *Canadian Triassic ammonoid faunas*. Geological Survey of Canada, Bulletin, **467**.

URDY, S., GOUDEMAND, N., BUCHER, H. & CHIRAT, R. 2010. Allometries and the morphogenesis of the molluscan shell: A quantitative and theoretical model. *Journal of Experimental Zoology, Part B: Molecular and Developmental Evolution*, **314B**, 280–302, doi:10.1002/jez.b.21337.

VAN VALEN, L. 1974. Multivariate structural statistics in natural history. *Journal of Theoretical Biology*, **45**, 235–247.

VILLIER, L. & KORN, D. 2004. Morphological disparity of ammonoids and the mark of Permian mass extinctions. *Science*, **306**, 264–266, doi:10.1126/science.1102127.

WANG, Y. & WESTERMANN, G.E.G. 1993. Paleoecology of Triassic ammonoids. *Geobios*, **26**, 373–392, doi:10.1016/S0016-6995(06)80391-8.

WARE, D., JENKS, J.F., HAUTMANN, M. & BUCHER, H. 2011. Dienerian (Early Triassic) ammonoids from the Candelaria Hills (Nevada, USA) and their significance for palaeobiogeography and palaeoceanography. *Swiss Journal of Geosciences*, **104**, 161–181, doi:10.1007/s00015-011-0055-3.

WESTERMANN, G.E.G. 1966. Covariation and taxonomy of the Jurassic ammonite, Sanninia adicra (Waagen). *Neues Jahrbuch für Geologie und Paläontologie, Abhandlungen*, **124**, 289–312.

WESTERMANN, G.E.G. 1971. *Form, structure and function of shell and siphuncle in coiled Mesozoic ammonoids*. Royal Ontario Museum, Toronto, 39pp.

WESTERMANN, G.E.G. 1996. Ammonoid life and habitat. *Ammonoid Paleobiology*, **13**, 607–707.

Received 5 July 2012; revised typescript accepted 25 September 2012.
Scientific editing by Philip Donoghue.